

# Tempering of hard mixture of bainitic ferrite and austenite

C. Garcia-Mateo, M. Peet, F. G. Caballero and H. K. D. H. Bhadeshia

Recent work has shown that bainitic ferrite plates produced by transformation at low temperatures can be as thin as 20 nm with a hardness in excess of 650 HV30, tensile strength  $\sim 2.3$  GPa and toughness  $\sim 30$  MPa m<sup>1/2</sup>. Because these properties rely on the fine scale of the microstructure, a study has been carried out in relation to the tempering resistance of steel over the temperature range 350–750°C. It is found that significant softening occurs only after the plates of ferrite begin to coarsen. The coarsening process is hindered by the intense precipitation of carbides resulting from decomposition of the carbon enriched retained austenite. The carbides themselves lead to some precipitation strengthening during the early stages of tempering. The ferrite is found to contain excess carbon, beyond its solubility limit, and X-ray analysis indicates that the carbon is associated with heterogeneous strains in the microstructure. It does not readily precipitate until the onset of substantial recovery during annealing. MST/5982

**Keywords:** Bainite, Carbides, Tempering, Retained austenite, Phase transformations, Kinetics

*Dr Garcia-Mateo, Mr Peet and Professor Bhadeshia (hkdb@cus.cam.ac.uk) are in the Department of Materials Science and Metallurgy, University of Cambridge, Pembroke Street, Cambridge CB2 3QZ, UK and Dr Caballero is at the Centro Nacional de Investigaciones Metalúrgicas (CENIM), Consejo Superior de Investigaciones Científicas (CSIC), Avda. Gregorio del Amo, 8, 28040 Madrid, Spain. Manuscript received 22 September 2003; accepted 13 January 2004.*

© 2004 IoM Communications Ltd. Published by Maney for the Institute of Materials, Minerals and Mining.

## Introduction

It has been discovered that bainite with an ultimate tensile strength in excess of 2.3 GPa and a toughness of  $\sim 30$  MPa m<sup>1/2</sup> can be obtained in high carbon, silicon rich steels by transformation at homologous temperatures which can be as low as  $T/T_m \approx 0.25$ , where  $T_m$  is the absolute melting temperature.<sup>1–3</sup> The reported combination of mechanical properties is a consequence of the very thin bainite plates (20–40 nm thickness) and the fine scale dispersion of austenite between the plates, obtained by transformation at the low temperature. Carbides are avoided in the microstructure by the judicious use of silicon as an alloying element. The details of the alloy design can be found in Ref. 1–3.

The hardness of this low temperature bainite can be as high as 700 HV30, exceeding that of the vast majority of as quenched martensitic microstructures. Indeed, it has been suggested that the hardness of martensite in steels becomes independent of carbon at  $\sim 800$  HV30, when a point is reached such that the resistance to dislocation motion becomes overwhelming.<sup>4–6</sup>

The strength of virgin martensite in steels relies mostly on the carbon concentration in solid solution.<sup>7</sup> Since the equilibrium solubility of carbon in body centred cubic iron at ambient temperature is negligible, the carbon rapidly precipitates when the martensite is tempered, leading to a great reduction in hardness.<sup>8</sup> Bainite in general tempers much more gently because it autotempers during the course of transformation.<sup>9</sup> Since its starting hardness is less than that of virgin martensite, it is not surprising that any change in hardness during tempering is small when compared with martensite. However, the starting hardness of the low temperature bainite is very high, so it was of interest to study its tempering behaviour, which is the subject of the present paper.

## Method

The chemical composition of the alloy studied, measured after homogenisation at 1200°C for 2 days in a vacuum chamber, was (wt-%) Fe–0.98C–1.46Si–1.89Mn–1.26Cr–0.26Mo–0.09V.

Cylindrical specimens of 3 mm in diameter and  $\sim 3$  cm in length were machined from the homogenised material. A hard bainite microstructure was obtained by austenitising for 15 min at 1000°C followed by isothermal transformation at 200°C for 10 days before quenching into water. The virgin microstructure was then tempered between 400 and 730°C for a variety of time periods. During tempering, the specimens were sealed in quartz tubes to protect against decarburisation, for heat treatments at 500°C and above.

Specimens for transmission electron microscopy were prepared by slicing 100  $\mu$ m discs from the 3 mm diameter rods. The discs were ground down to 50  $\mu$ m thickness using 1200 grit silicon carbide paper, for electropolishing at 50 V using a twin jet unit. The electrolyte consisted of 5% perchloric acid, 15% glycerol and 80% ethanol. Vickers hardness tests are reported as the average of at least three tests. The tests were conducted using a 30 kg load.

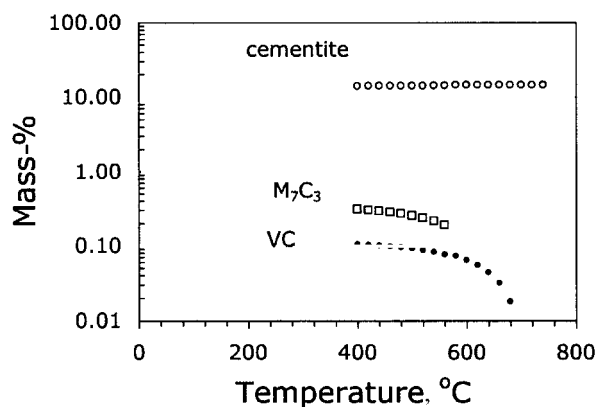
X-ray experiments were carried out using a Philips PPW1730 diffractometer and a scanning rate of  $0.1^\circ \text{ min}^{-1}$  over the range  $2\theta = 30–110^\circ$ , with unfiltered Cu  $K_\alpha$  radiation, and the system operating at 45 kV and 45 mA. Peak positions and widths of Bragg reflections were determined by a self-consistent profile fitting technique using the Pearson VII function. The fraction of retained austenite in the virgin microstructure was evaluated from the integrated intensities of the 111, 200, 220 and 311 austenite peaks and the 110, 002, 112 and 022 peaks of ferrite. By using these peaks it is possible to avoid bias owing to crystallographic texture.<sup>10</sup> The austenite carbon content was calculated making use of the following expression<sup>11</sup>

$$a_\gamma = 3.5780 + 0.033w_C + 0.00095w_{Mn} - 0.0002w_{Ni} + 0.0006w_{Cr} + 0.0056w_{Al} + 0.0031w_{Mo} + 0.0018w_V$$

where  $a_\gamma$  is the lattice parameter of austenite in Å, and  $w_i$  is the concentration of element  $i$  in wt-%. Similarly, for ferrite<sup>12</sup>

$$a_\alpha = 2.8664 + \frac{(a_{Fe} - 0.279x_C)^2(a_{Fe} + 2.496x_C) - a_{Fe}^3}{3a_{Fe}^2} - 0.03x_{Si} + 0.06x_{Mn} + 0.07x_{Ni} + 0.31x_{Mo} + 0.05x_{Cr} + 0.096x_V$$

where  $x_i$  is the concentration in mole fraction and



**1** Calculated equilibrium mass fractions of carbides as function of tempering temperature: note that these are fractions expected following prolonged annealing

$a_{\text{Fe}} = 2.8664 \text{ \AA}$  (0.28664 nm) is the lattice parameter of ferrite in pure iron.

Cohen's method<sup>13</sup> was applied to obtain accurate values of the lattice parameters of austenite and ferrite. The parameters calculated from individual peaks were plotted against  $\cos^2\{\theta\}/\sin\{\theta\}$ , and the precise lattice parameters  $a_x$  and  $a_y$  were obtained by extrapolating the diffraction angle  $\theta$  to  $90^\circ$ , with the highest angles being given the greatest weights in the extrapolation. The weighting was carried out by conducting regression analysis on a data set containing just one point for the lowest  $\theta$  value, two identical points for the next  $\theta$  value and so on. This is because the largest  $2\theta$  are associated with smaller errors in the calculation of lattice parameters. Because of the experimental setup, the amount of specimen surface scanned at large  $\theta$  is smaller than at lower angles. X-ray experiments were carried out to assess whether this matters, by making measurements with a rotating specimen to increase the effective area scanned, but this made no significant difference to the measured parameters or volume fractions.

Numerous precipitates were formed during tempering. Individual particles were identified to be cementite using electron diffraction in a transmission electron microscope. However, the number density of particles was very large, so X-ray diffraction was also used. For the latter method, the specimens (cylinders, 10 mm length, 3 mm diameter) were dissolved in 2% nital over a period of several days in order to extract the carbides. When the matrix had dissolved, the suspension was filtered through a 0.2  $\mu\text{m}$  polycarbonate membrane filter. This confirmed the precipitates to be cementite during tempering at 550 and 600°C, but good residues could not be extracted following the lower tempering temperatures when the carbides were fine.

It is possible that alloy carbides such as VC<sub>0.88</sub> and M<sub>7</sub>C<sub>3</sub> (where M denotes metal atoms, but particularly Cr) are also possible, particularly during tempering at temperatures in excess of 550°C where substitutional atoms become mobile. These were not found, but that is not to suggest that they are not present in the microstructure. Their expected phase fractions are very low compared with cementite, as shown in Fig. 1, so they would not be easy to detect. The calculations were carried out using MTDATA, a commercially available computer program from the National Physical Laboratory, Teddington, UK together with the Scientific Group Thermodata Europe (SGTE) database. They allowed the existence of ferrite, cementite, VC<sub>0.88</sub> and M<sub>7</sub>C<sub>3</sub> and all the elements listed above in the chemical composition of the alloy.

The X-ray data from the microstructure were also analysed for non-uniform strains. Diffraction peaks are broadened by the presence of non-uniform strains that systematically shift atoms from their ideal positions, and the

finite crystallite size (coherently diffracting domain). These two effects have a different dependence on the value of  $\theta$ , which is the Bragg angle.<sup>14</sup> The non-uniform strain effect can therefore be separated, since the slope of a plot of  $\beta_{\text{hkl}} \cos\{\theta_{\text{hkl}}\}$  versus  $4 \sin\{\theta_{\text{hkl}}\}$  is equal to the strain  $\varepsilon$ .<sup>14</sup> The parameter  $\beta$  is the measured peak broadening; it is defined as the width of a rectangle with the same area and height as the diffraction peak. In general,  $\varepsilon$  is proportional to the square root of the dislocation density.

Dilatometric analysis was carried out in an Adamel Lhomargy DT1000 high resolution dilatometer, on specimens of 2 mm in diameter and 12 mm in length, in order to measure the  $A_{c1}$  transformation temperature.

## Initial microstructure

The untempered microstructure, consisting of a mixture of bainitic ferrite and carbon enriched retained austenite, was produced by isothermal transformation at 200°C for 10 days after austenitising at 1000°C for 15 min. Quantitative data are summarised in Table 1.

The morphological details have been discussed elsewhere,<sup>3</sup> but it is useful to summarise the relevant points here. The austenite is present in two forms, as thin films between the bainitic ferrite platelets and as coarser blocks between sheaves of bainite. Figure 2a illustrates the blocks, whereas the transmission electron micrographs in Fig. 2b show films of austenite interspersed with fine plates of bainitic ferrite. The austenite is sufficiently enriched with carbon (Table 1) to remain stable during cooling to ambient temperature; martensite therefore does not form after the isothermal transformation heat treatment. Nevertheless, a very high hardness in excess of 600 HV30 is achieved, primarily due to the fine scale of the microstructure.<sup>3</sup> A selection of transmission electron micrographs was used to determine the true plate thickness  $t$  by measuring the mean linear intercept  $\bar{L}_T = \pi/t$ , in a direction normal to the plate length. The thickness  $t$  is related to the mean linear intercept measured using randomly oriented test lines, and is given by the relationship  $\bar{L} = 2t$ , but  $\bar{L}_T$  is easier to measure since it is rare in transmission electron micrographs that entire plates of bainite can be imaged. The thickness of the ferrite plates in the initial microstructure was measured to be extremely fine, 35 nm.

It can be noted from Table 1 that the bainitic ferrite contains a carbon concentration which is well in excess of equilibrium, as determined from the measured lattice parameters. This is discussed below in the context of the non-uniform strain data and the changes that occur during the course of tempering.

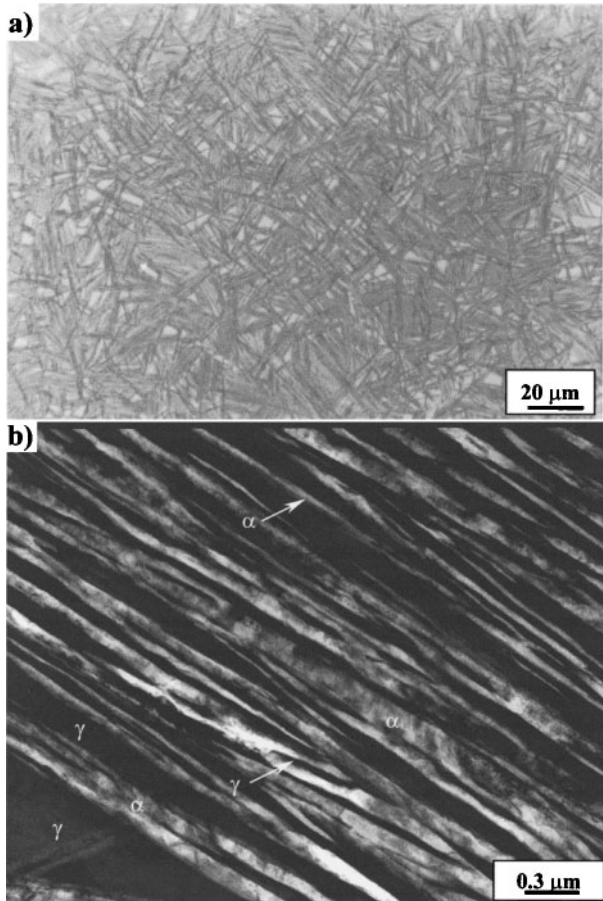
## Tempering resistance

The virgin microstructure was tempered at a variety of temperatures below the dilatometrically measured  $A_{c1}$  temperature of 804°C (measured for a heating rate of 0.05 Ks<sup>-1</sup>), and for different periods of time. The hardness as a function of the tempering conditions is plotted in Fig. 3a. There is at first a slight increase in hardness, with

**Table 1** Measured data\* for initial microstructure

$V_\gamma$	$x_\gamma$ , wt-%	$x_\alpha$ , wt-%	HV30	$t$ , nm
0.31 ± 0.01	1.5 ± 0.1	0.3 ± 0.07	619 ± 5	35 ± 3

\* $V_\gamma$  is volume fraction of austenite,  $x$  represents carbon concentration of phase identified by subscript and  $t$  is thickness of bainitic ferrite plates.



a blocky austenite between sheaves of bainite; b austenite films interspersed with fine plates of bainitic ferrite

## 2 Optical and transmission electron micrographs showing virgin microstructure obtained by isothermal transformation at 200°C for 10 days

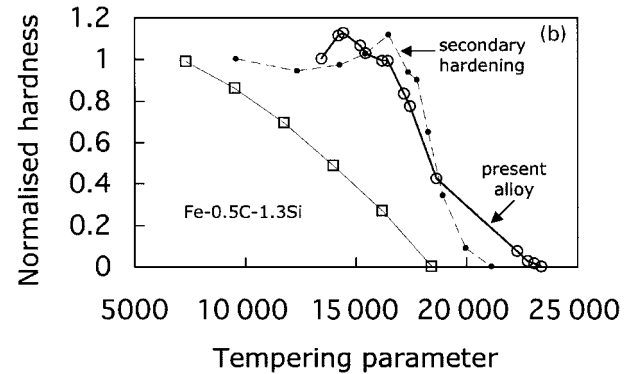
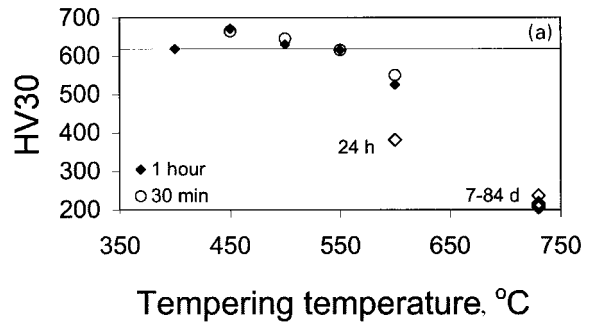
substantial softening occurring only when the tempering temperature exceeds  $\sim 500^\circ\text{C}$ .

Figure 3b shows a plot of the normalised hardness of a variety of steels versus the tempering parameter. The latter is defined as  $T(20 + \log t)$ , where  $T$  is expressed in K and  $t$  in h. The normalised hardness is given by  $(H - H_{\min}) / (H_{\max} - H_{\min})$ , where  $H$ ,  $H_{\max}$  and  $H_{\min}$  represent the hardness, untempered hardness and fully softened hardness, respectively. The reason for presenting the data in this way is to allow a comparison of the tempering resistance of the bainitic steel against that of a high silicon, quenched and tempered martensitic steel (Fe-0.5C-1.3Si Ref. 15) and a high silicon, secondary hardening steel (Fe-0.34C-5.08Cr-1.43Mo-0.92V-0.4Mn-1.07Si Ref. 16). The minimum and maximum values of the hardnesses of the three steels for the tempering conditions used are stated in Table 2.

It is apparent from Fig. 3 that the bainitic steel has a very high resistance to tempering, much higher than that of the martensitic alloy, and even compares well against the secondary hardening steel. The reasons for this are discussed below in the context of the metallographic studies.

**Table 2** Maximum and minimum hardness values  $H$  as used in calculation of normalised hardness

Alloy	$H_{\max}$	$H_{\min}$
Bainitic steel	619	206
Martensitic steel	820	245
Secondary hardening steel	510	248



**3 a** Vickers hardness as function of tempering temperature and time: each value represents mean of three measurements, with scatter of typically less than  $\pm 5$  HV30, and horizontal line represents virgin microstructure; **b** comparison of temper resistance of present alloy with that of Fe-0.5C-1.3Si quenched and tempered martensitic steel, and secondary hardening steel

## Carbon in bainitic ferrite

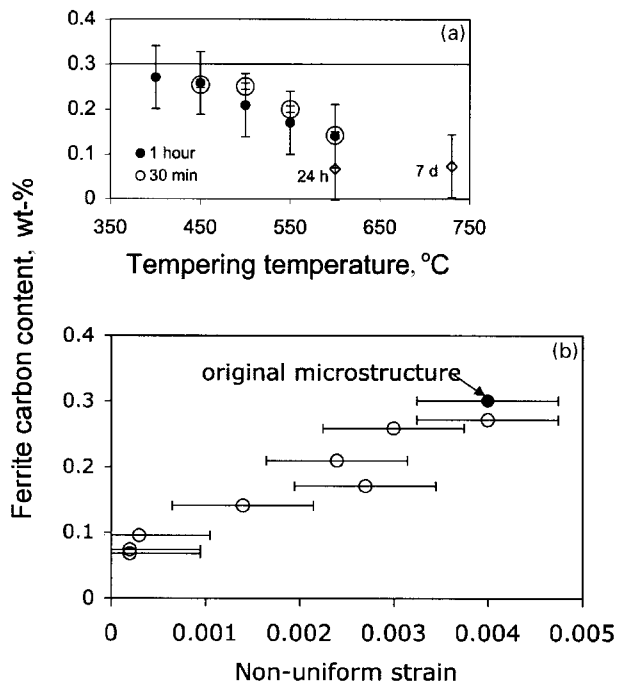
Previous studies have shown that the bainite generated after low temperature transformation contains a concentration of carbon which is well above that expected from equilibrium.<sup>2</sup> Indeed, a supersaturation of carbon in bainitic ferrite has been demonstrated in lower carbon bainitic steels using the atom probe.<sup>17,18</sup> In all these studies, it has been suggested that the excess carbon is located at defects such as dislocations within the ferrite lattice.

It is possible, using X-ray analysis, to measure the heterogeneous strains present in ferrite and to relate these to the carbon concentration in the ferrite. The measured carbon content in the ferrite from X-ray diffraction analysis is shown in Fig. 4a as a function of the tempering conditions. Like the hardness (Fig. 3a), the carbon content remains nearly unaltered up to temperatures as high as  $550^\circ\text{C}$ . It is at first surprising that the carbon does not precipitate as cementite or other carbides.

Figure 4b shows the carbon concentration as a function of the measured non-uniform strain. It is clear that there is a strong correlation, confirming that the carbon is likely to be located at defects. This might also explain why it does not precipitate easily until the non-uniform strains are relieved by annealing. It has long been known that carbon which is segregated to dislocations is stabilised against precipitation, because the segregation itself leads to a reduction in free energy.<sup>19</sup>

## Microstructural changes

Tempering for 1 h at  $400^\circ\text{C}$  does not introduce any perceptible change in the original microstructure, consistent with the hardness, non-uniform strain and composition



4 a carbon concentration in bainitic ferrite as function of tempering conditions; b ferrite carbon concentration as function of non-uniform strain

data presented above. The microstructure still consists of extremely fine plates of ferrite, with thin films and blocks of retained austenite, as shown in Fig. 5a. The X-ray determined fraction of austenite in this condition is  $0.29 \pm 0.01$ ,

essentially the same as that in the virgin microstructure (Table 1). Further tempering ( $450^\circ\text{C}$ ) actually leads to a slight increase ( $\sim 50$  HV30) in hardness, as the retained austenite decomposes mostly by the precipitation of fine carbides (Fig. 5b). The X-ray determined retained austenite fraction is  $\sim 0.02$ , a figure which is uncertain because only two small austenite peaks could be recorded. There is no perceptible change in the overall plate microstructure of the bainite.

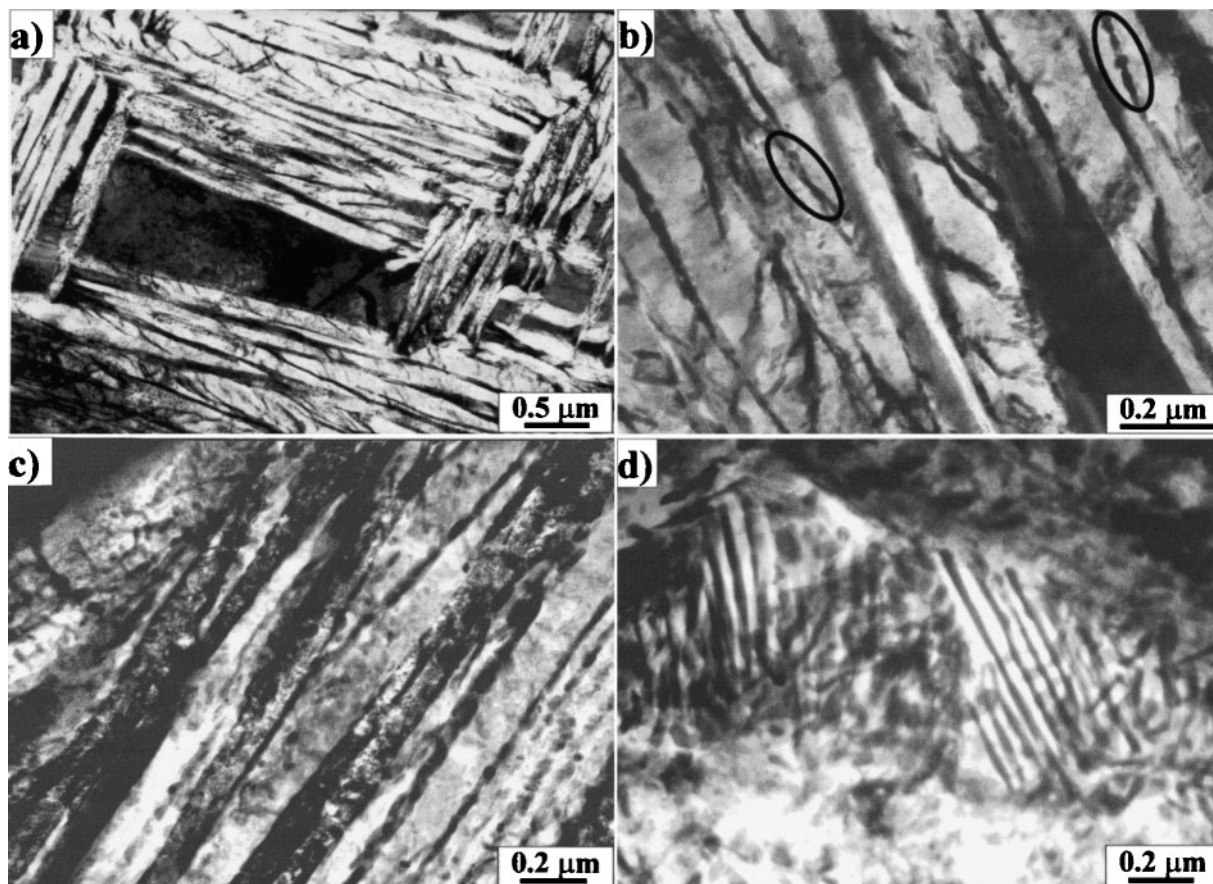
The hardness is maintained between 615 and 640 HV30 during tempering at 500 and  $550^\circ\text{C}$ , in spite of some recovery (Fig. 5c). The retained austenite has at this stage completely decomposed, the larger regions decomposing into pearlite (Fig. 5d). By contrast, fine regions of austenite decompose into discrete particles of carbide and ferrite because there is insufficient space to establish the cooperative growth of pearlite.

Tempering at temperatures below  $\sim 550^\circ\text{C}$  leads to rather small changes in the thickness of the bainite plates. The plates in the virgin microstructure are  $\sim 35$  nm in thickness. This changes to  $45 \pm 4$  nm and  $49 \pm 4$  nm following tempering at  $450^\circ\text{C}$  and  $550^\circ\text{C}$  for 30 min in each case.

It is at  $600^\circ\text{C}$  when major changes begin to occur in all of the measured data. The microstructure after 1 h at  $600^\circ\text{C}$  is generally coarser (Fig. 6a), with further coarsening occurring during prolonged tempering for 1 day (Fig. 6b). Only remnants of the original plate microstructure remain on tempering at  $700^\circ\text{C}$  for 7 and 42 days (Fig. 6c and d), with considerable signs of recovery, if not recrystallisation.

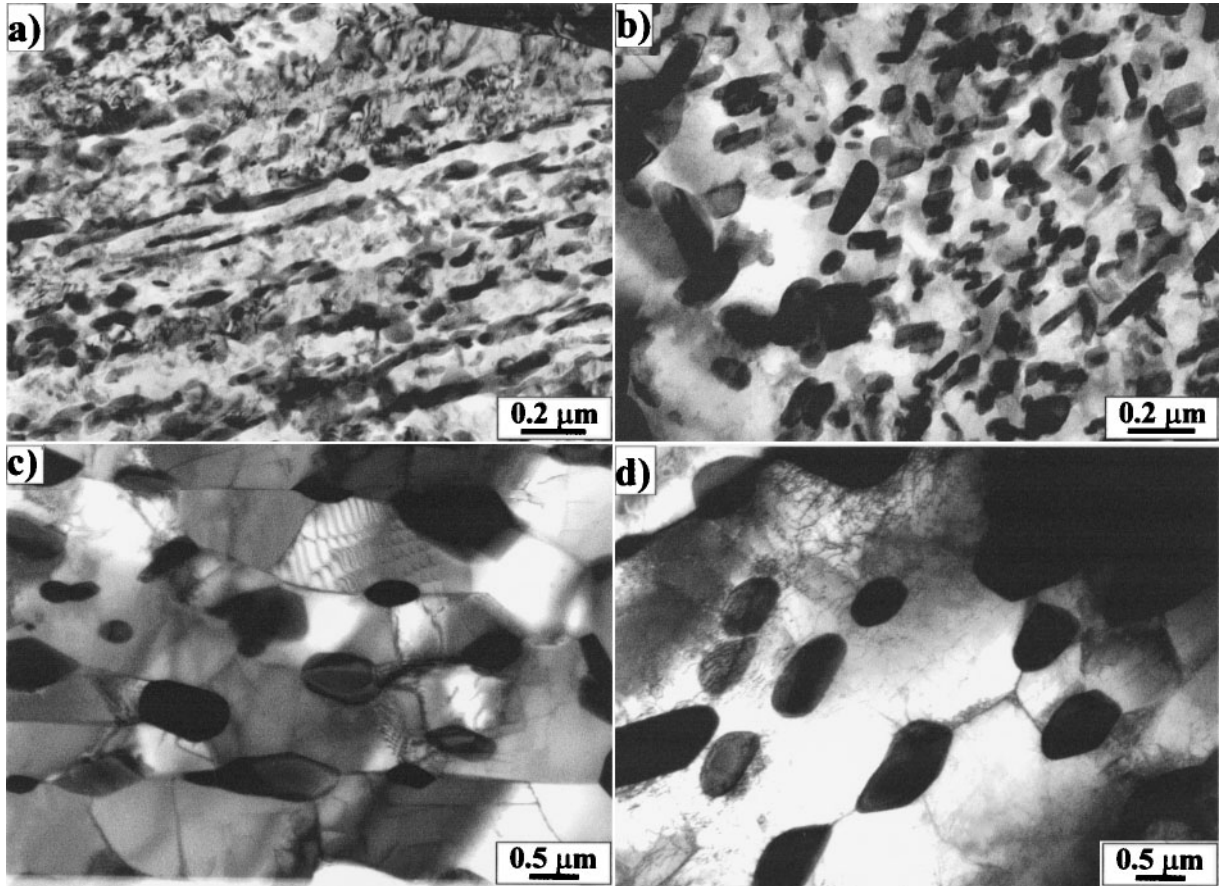
## Summary

It has been demonstrated in earlier studies<sup>2,3</sup> that much of the strength (1700 MPa out of 2300 MPa) of the virgin



a  $400^\circ\text{C}$ , 1 h; b  $450^\circ\text{C}$ , 30 min, showing some fine carbide precipitation; c  $550^\circ\text{C}$ , 30 min; d  $550^\circ\text{C}$ , 1 h

## 5 Microstructures following tempering



a 600°C, 1 h; b 600°C, 1 day; c 730°C, 7 days; d 730°C, 42 days

## 6 Microstructures following tempering

microstructure comes from the fine size of the bainite plates in the alloy investigated in the present work. The above results suggest that the resistance of this microstructure to tempering arises because it is very difficult for the plate microstructure to coarsen owing to the intense precipitation of carbides. These carbides form from the carbon enriched austenite between the bainitic ferrite plates in the virgin microstructure, and hence are ideally located to prevent the plate coarsening process.

The carbides themselves lead to some precipitation strengthening as indicated by the rise in hardness during the early stages of tempering. It is not surprising, therefore, that the decomposition of austenite itself does not lead to any overall softening.

There is excess carbon present in the ferrite, and because this is associated with heterogeneous strains, it does not precipitate until there is substantial recovery in the microstructure.

## Acknowledgements

The authors are grateful to the Engineering and Physical Sciences Research Council for supporting this research. They are also grateful to Miss P. Swannell for her general help with the experiments and to Dr M. Vickers for help with the interpretation of X-ray data. One of the authors (FGC) would like to thank the Spanish Ministerio de Ciencia y Tecnología for financial support in the form of a Ramón y Cajal award (Programa RyC 2002).

## References

1. F. G. CABALLERO, H. K. D. H. BHADESHIA, K. J. A. MAWELLA, D. G. JONES, and P. BROWN: *Mater. Sci. Technol.*, 2002, **18**, 279–284.
2. C. GARCIA-MATEO, F. G. CABALLERO, and H. K. D. H. BHADESHIA: *J. Phys. Colloq.*, 2003, **112**, 285–288.
3. C. GARCIA-MATEO, F. G. CABALLERO, and H. K. D. H. BHADESHIA: *ISIJ Int.*, 2003, **43**, 1238–1243.
4. H. K. D. H. BHADESHIA and D. V. EDMONDS: *Met. Sci.*, 1983, **17**, 411–419.
5. H. K. D. H. BHADESHIA and D. V. EDMONDS: *Met. Sci.*, 1983, **17**, 420–425.
6. C. H. YOUNG and H. K. D. H. BHADESHIA: *Mater. Sci. Technol.*, 1994, **10**, 209–214.
7. J. W. CHRISTIAN: in ‘Strengthening methods in crystals’, (ed. A. Kelly and R. Nicholson), 261–329; 1971, Amsterdam, Elsevier.
8. G. R. SPEICH and W. C. LESLIE: *Metall. Trans.*, 1972, **3**, 1043–1054.
9. H. K. D. H. BHADESHIA: ‘Bainite in steels’, 2nd edn; 2001, London, The Institute of Materials.
10. M. J. DICKSON: *J. Appl. Crystallogr.*, 1969, **2**, 176–180.
11. D. J. DYSON and B. HOLMES: *J. Iron Steel Inst.*, 1970, **208**, 469–474.
12. H. K. D. H. BHADESHIA, S. A. DAVID, J. M. VITEK, and R. W. REED: *Mater. Sci. Technol.*, 1991, **7**, 686–698.
13. B. D. CULLITY and S. R. STOCK: ‘Elements of X-ray diffraction’, 3rd edn; 2001, New York, Prentice Hall.
14. G. K. WILLIAMSON and W. H. HALL: *Acta Metall.*, 1953, **1**, 22–31.
15. E. C. BAIN: ‘The alloying elements in steel’, 239; 1939, Cleveland, OH, American for Society Metals.
16. G. P. CONTRACTOR, E. G. SCHEMPP, and W. A. MORGAN: *Trans. AIME*, 1969, **54**, 208–219.
17. H. K. D. H. BHADESHIA and A. R. WAUGH: ‘Solid–solid phase transformations’, 993–998; 1981, Warrendale, PA, TMS.
18. H. K. D. H. BHADESHIA and A. R. WAUGH: *Acta Metall.*, 1982, **30**, 775–784.
19. D. KALISH and M. COHEN: *Mater. Sci. Eng.*, 1970, **6**, 156–166.